

Strontium ranelate improves the interaction of osteoblastic cells with titanium substrates: Increase in cell proliferation, differentiation and matrix mineralization

William Querido^{1,2,3}, Marcos Farina², and Karine Anselme^{1,*}

¹Institut de Sciences des Matériaux de Mulhouse; CNRS UMR7361; Université de Haute-Alsace; Mulhouse, France; ²Instituto de Ciências Biomédicas; Universidade Federal do Rio de Janeiro; Rio de Janeiro, Brazil; ³Instituto de Biofísica Carlos Chagas Filho; Universidade Federal do Rio de Janeiro; Rio de Janeiro, Brazil

Keywords: biomineralization, cell/material interaction, osteoblastic cells, strontium ranelate, surface topography

We describe direct effects of strontium ranelate on the interaction of osteoblastic cells with different titanium substrates. Our goal was to better understand the potential of this drug for improving the efficacy of bone implants. Treatment was done with 0.12 and 0.5 mM Sr^{2+} of strontium ranelate in cell culture. We analyzed cell response to the drug on titanium substrates with surface topographies obtained using acid etching, electro-erosion processing, sandblasting, and machine-tooling. Treatment preserved the initial cell adhesion to the substrates, cell shape parameters (area, aspect ratio, circularity, and solidity), and the orientation of cells on grooved surfaces. However, both concentrations of the drug increased cell proliferation in all substrates. Moreover, a dose-dependent increase in alkaline phosphatase activity and in the production of mineralized matrix with typical features of bone tissue was shown. The observed effects were similar in the different substrates. In conclusion, strontium ranelate improved the interaction of osteoblastic cells with titanium substrates, increasing cell proliferation and differentiation into mature osteoblasts and the production of bone-like mineralized matrix for all substrates. This study highlights a promising role of strontium ranelate on enhancing the clinical success of bone implants, particularly in patients with osteoporosis.

Introduction

The clinical success of bone implants is highly dependent on the proper integration of the biomaterial into the regenerated bone tissue. This integration occurs through the adhesion, proliferation, and differentiation of osteoblastic cells followed by the production of mineralized matrix directly on the surface of the biomaterial.¹⁻⁴ Many strategies can be used aiming to improve implant osseointegration. A promising strategy on the material side is the manipulation of the surface characteristics of implants, which allows creating a variety of surface topographies that can enhance cell and tissue responses.^{2,5,6} In particular, materials with grooved surfaces seem to be of interest because they induce contact guidance of the cells (i.e., cells tend to align in the direction of the grooves), which may have positive effects on bone growth.^{7,8}

A particular strategy to improve implant osseointegration is the association of biomaterials with molecules involved in osteoblastic cell adhesion, proliferation, and/or differentiation, aiming to enhance the interaction of cells with the biomaterial and thus

the quality of the tissue/material interface.^{1,9-11} Among these molecules, members of the bone morphogenic protein (BMP) family, such as BMP-2 and BMP-7, are of special interest because they can stimulate osteoblastic cell differentiation and promote bone tissue formation.¹²⁻¹⁴

Strontium ranelate is a promising drug used for treating postmenopausal osteoporosis. It has a unique dual mode of action, simultaneously increasing bone formation by osteoblasts and decreasing bone resorption by osteoclasts, thus improving bone strength.¹⁵⁻¹⁷ In cell cultures, strontium ranelate increased osteoblastic cell proliferation,^{18,19} differentiation,^{20,21} and the production of mineralized nodules.^{21,22} In postmenopausal women with osteoporosis, long-term treatment reduced the risk of nonvertebral, hip, and vertebral bone fractures.^{23,24} Moreover, systemic administration of strontium ranelate enhanced the volume and microarchitecture of the bone tissue surrounding implants, improving implant fixation and osseointegration.²⁵⁻²⁷ Further studies are necessary to better understand the potential of strontium ranelate for improving the efficacy of bone implants.

© William Querido, Marcos Farina, and Karine Anselme

*Correspondence to: Karine Anselme; Email: karine.anselme@uha.fr

Submitted: 06/24/2014; Revised: 01/20/2015; Accepted: 03/05/2015

<http://dx.doi.org/10.1080/21592535.2015.1027847>

This is an Open Access article distributed under the terms of the Creative Commons Attribution-Non-Commercial License (<http://creativecommons.org/licenses/by-nc/3.0/>), which permits unrestricted non-commercial use, distribution, and reproduction in any medium, provided the original work is properly cited. The moral rights of the named author(s) have been asserted.

The goal of this study was to evaluate direct effects of strontium ranelate on the interaction of osteoblastic cells with different titanium substrates. In particular, we investigated effects on cell adhesion, proliferation, and differentiation into mature osteoblasts and on the production of bone-like mineralized matrix on substrates with different surface topographies, obtained using acid etching (TAN), electro-erosion processing (TE0N), sandblasting (TS0N), and machine-tooling (TU0N) (Figs. 1A–D). We also analyzed cell shape and the orientation of cells on grooved surfaces. The results of this study highlight a promising role of strontium ranelate for improving the clinical success of bone implants, particularly in patients with osteoporosis.

Results

In all analyzed conditions, cells were well adhered and spread on the different substrates after 24 hours in culture, often presenting a stellate shape with distinct prolongations (Figs. 2A–L). Further analysis showed no significant differences in morphological parameters of the cells (area, aspect ratio, circularity, and solidity) between control and treated samples in any of the substrates (Figs. 3A–D). Moreover, on

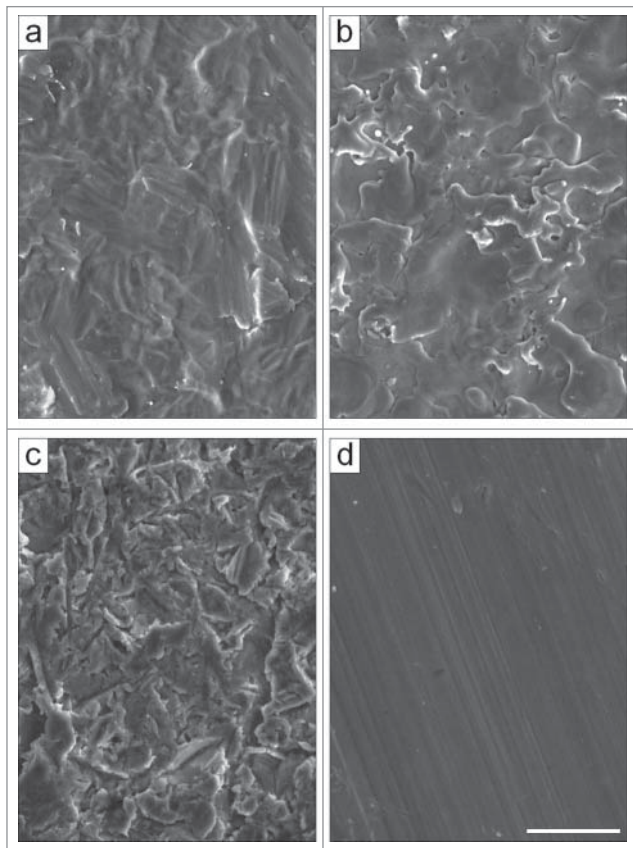


Figure 1. Scanning electron micrographs of the pure titanium substrates. The different surface topographies were obtained by using: (A) acid etching (TAN), (B) electro-erosion processing (TE0N), (C) sandblasting (TS0N), and (D) machine-tooling (TU0N). Note the parallel grooves on the TU0N substrates. Scale bar: 25 μm .

TU0N substrates, cells were preferentially aligned with the direction of the grooves, with a similar distribution seen in control and treated samples (Figs. 4A–C).

The number of cells adhered after 4 hours showed no significant differences between control and treated samples in any of the substrates (Fig. 5A). After 24 hours, however, we noticed a significant increase in the number of cells in treated samples compared with control in TAN and TE0N substrates (Fig. 5B), reflecting an increase in the initial proliferation of the cells.

Further analysis showed that strontium ranelate not only had no toxic effects on the cells, but significantly increased cell proliferation rates in both treated samples on all substrates, particularly from 7 to 21 days in culture (Figs. 6A–D). Treatment with both concentrations of the drug increased cell proliferation quite consistently after 7 days in cultures. After 21 days, however, this increase was less consistent: in TAN substrates, only cells treated with 0.12 mM Sr^{2+} showed an increase; in TE0N, an increase was only seen on cells treated with 0.5 mM Sr^{2+} ; and in TS0N and TU0N, both concentrations of the drug increased cell proliferation.

The alkaline phosphatase (ALP) activity of treated cells had significantly higher values in all substrates (Figs. 7A–D), indicating an increase in the differentiation of the cells into mature osteoblasts. This increase was especially marked after 21 days in culture, occurring mostly in a dose-dependent manner.

An extensive mineralized matrix was formed in all analyzed conditions after 28 days in culture, presenting typical mineralized nodules that were readily stained with Alizarin red (Figs. 8A–L). By simple visual inspection, we noticed that this matrix seemed more developed in treated samples, especially in those treated with 0.5 mM Sr^{2+} . Quantification of Alizarin red extracted from the stained cultures confirmed that the drug induced a significant dose-dependent increase in the formation of mineralized matrix in all substrates (Fig. 9A). We also found that the concentration of calcium left in the medium after culture of treated samples was significantly reduced in all substrates (Fig. 9B), which is in agreement with the increase in deposition of calcium phosphate minerals in the matrix.

The mineralized matrix produced in all analyzed conditions presented similar bone-like characteristics. Typically, we saw well-developed cell layers along with numerous globular accretions associated with an extensive mesh of randomly oriented fibrils (Fig. 10A), as often seen in the newly formed native bone. Analysis of the matrix by Fourier transform infrared spectroscopy (FTIR) confirmed its bone-like nature, showing bands of PO_4^{3-} and CO_3^{2-} from the carbonated apatite mineral and of Amide I and II from the organic matrix proteins (Fig. 10B).

Discussion

Strontium ranelate was shown to improve the osseointegration of titanium implants *in vivo*.^{25–27} In these studies, the authors evaluated the surrounding bone by micro-CT and biomechanical testing. However, they did not analyze the cellular components of the bone/implant interactions. Because of the dual mode of action of strontium ranelate,^{15–17} it is difficult to assess in these

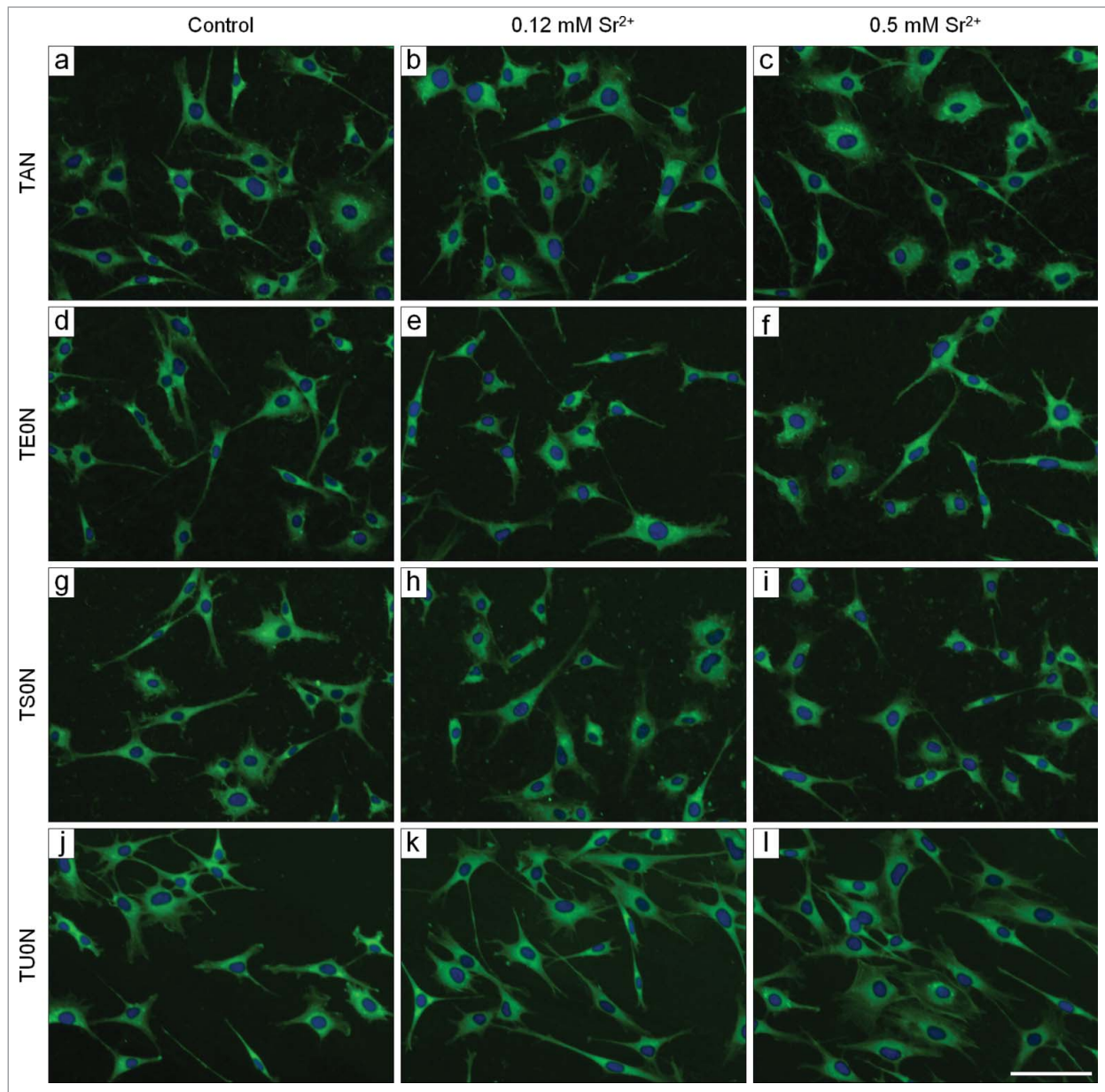


Figure 2. Fluorescence micrographs of cells labeled with FITC-phalloidin and DAPI. Cells were cultured for 24 hours. The actin cytoskeleton is shown in green and the nuclei in blue. The cells were well adhered and spread in all analyzed conditions. They often presented a stellate shape with distinct prolongations. Scale bar: 50 μm .

in vivo studies if the obtained results were directly related to an increase in bone formation. In our study, using an *in vitro* osteoblastic cell culture system, we provide evidence of a direct effect of strontium ranelate in the interaction of osteoblastic cells with biomaterials with different topographies, presenting new data on how this drug may act on improving implant osseointegration. We show that treatment with strontium ranelate has clear positive effects on the behavior of osteoblastic cells cultured on different titanium substrates, increasing cell proliferation and differentiation into mature osteoblasts and the production of bone-like mineralized matrix. This study is of value to better

understand the promising role of strontium ranelate for improving the efficacy of bone implants.

The first interaction of cells with biomaterials occurs through the attachment, adhesion, and spreading of the cells on the surface of the material, which will subsequently influence cell proliferation and differentiation.¹ One way of accessing the quality of this interaction is by analyzing cell shape. In this study, we found that strontium ranelate induced no changes in morphological parameters of the cells, preserving a normal first interaction of the osteoblastic cells with the substrates. Moreover, no changes were found in the orientation of cells in the grooved substrates,

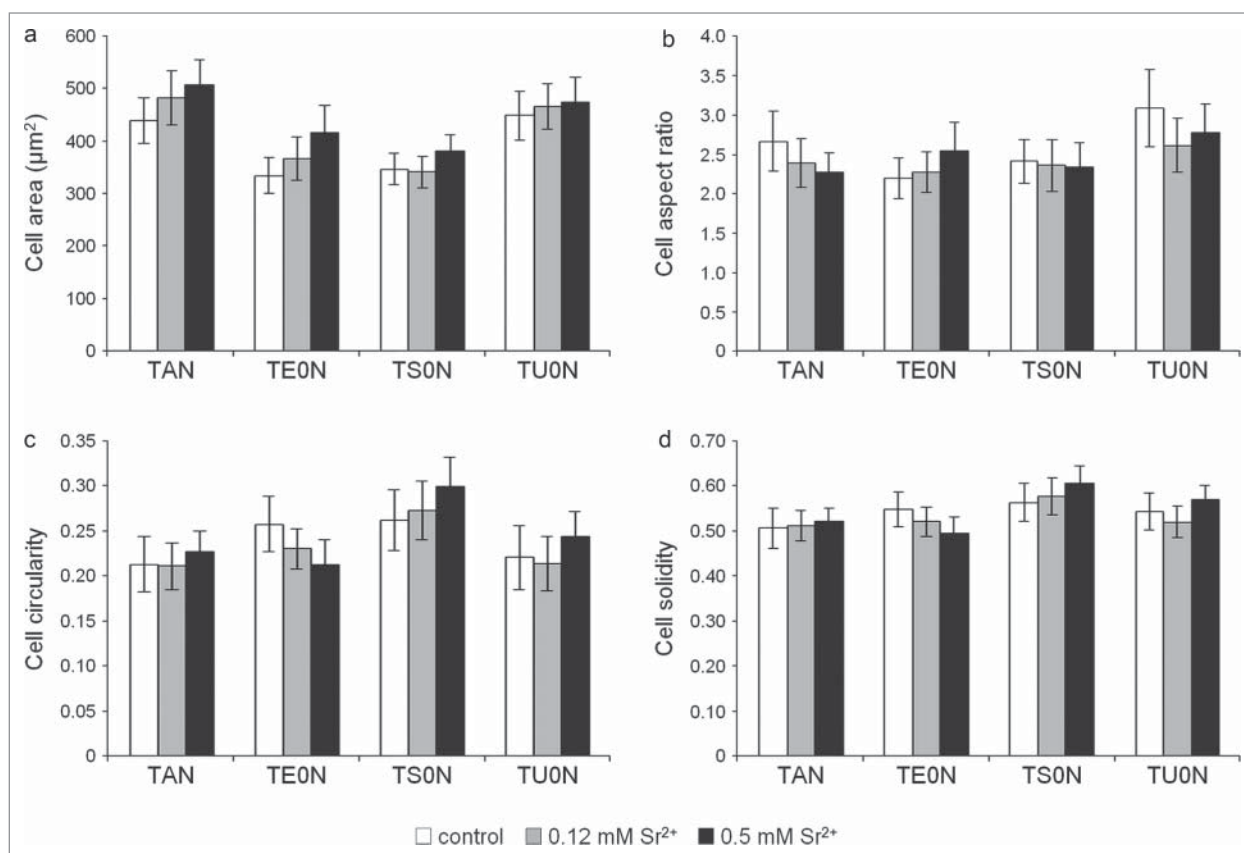


Figure 3. Analysis of the cell morphology. Individual cells labeled with FITC-phalloidin were analyzed with the ImageJ software after 24 hours in culture. The morphological parameters analyzed were: (A) cell area, (B) cell aspect ratio, (C) cell circularity, and (D) cell solidity. No significant differences were seen between control and treated samples in any substrate.

indicating that the drug also preserves the contact guidance induced by this type of material.⁸

We saw no differences in the initial adhesion of the cells to the substrates. We did, however, find that strontium ranelate increased cell proliferation rate in all substrates, indicating that

treatment may facilitate the development of osteoblastic cell layers directly on the surface of biomaterials. This improvement in surface colonization by bone-forming cells may be seen as an important step toward the integration of the biomaterial into the regenerated bone tissue.^{3,4}

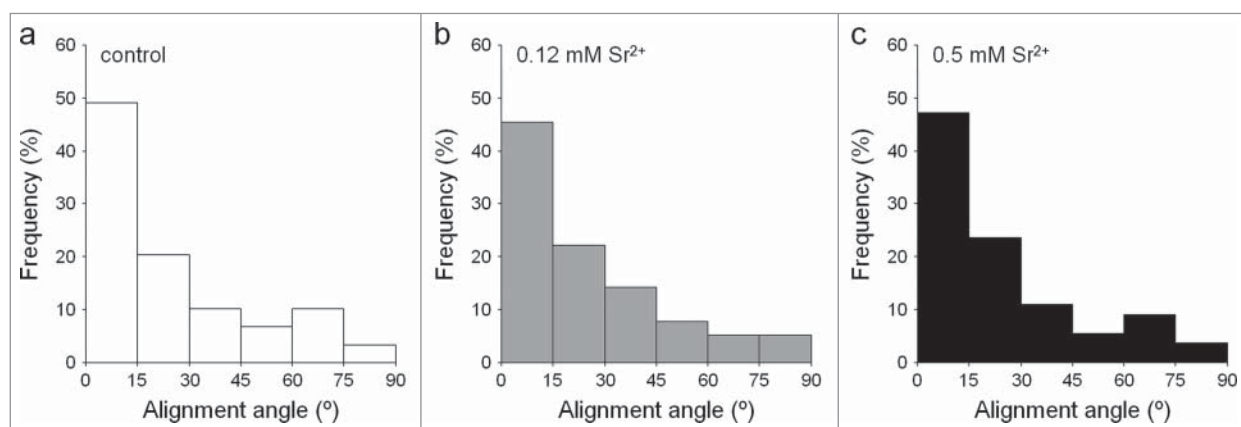


Figure 4. Analysis of cell orientation on TU0N substrates. Individual cells labeled with FITC-phalloidin were analyzed with the ImageJ software after 24 hours in culture. Alignment of the cells with the parallel grooves of TU0N substrates was quantified from 0° (perfectly aligned) to 90° (exactly perpendicular). In control and treated samples, the cells were preferentially aligned with the direction of the grooves, presenting a similar distribution.

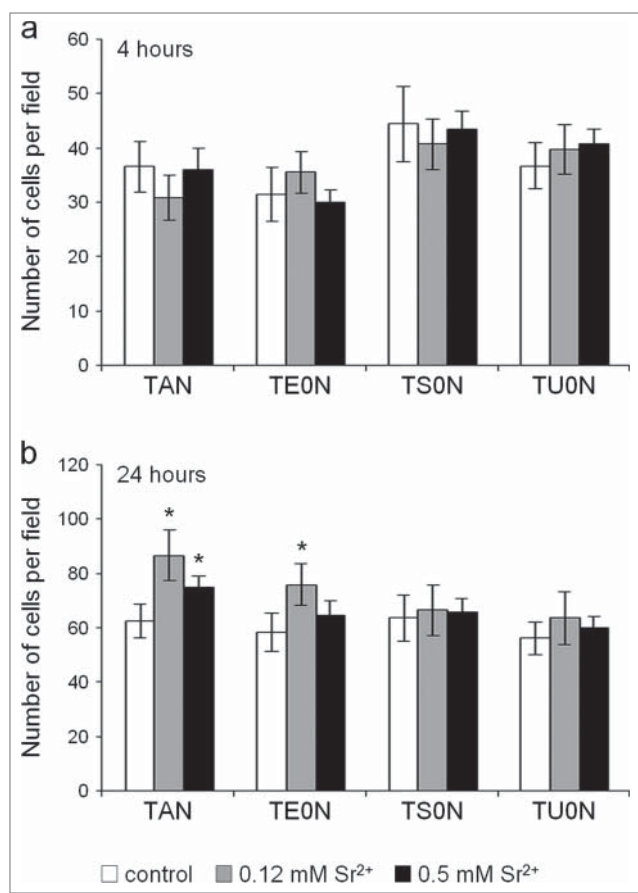


Figure 5. Analysis of the number of cells adhered on the substrates. The nuclei labeled with DAPI were counted with the ImageJ software in images taken using a 10× objective lens. (A) After 4 hours in culture, no significant differences were found between control and treated samples in any substrate. (B) After 24 hours, the number of cells in treated samples was higher than in control in TAN and TEON substrates, suggesting an increase in the initial cell proliferation. This increase showed a medium effect size on both substrates ($r \approx 0.3-0.5$). * $P < 0.05$ vs. control.

Strontium ranelate increased cell differentiation into mature osteoblasts, as seen by the marked increase in ALP activity in all substrates. A high ALP activity is one of the most typical markers of a more mature, matrix-synthesising osteoblastic phenotype.²⁸ This enzyme is especially related to initial phases of matrix mineralization. It functions both by increasing the local concentration of inorganic phosphate available to bone mineral deposition and by decreasing that of extracellular pyrophosphate, an inhibitor of mineral formation, thus promoting matrix mineralization.²⁹

Indeed, we found that strontium ranelate promoted the formation of mineralized matrix in all substrates. Moreover, this matrix had a typical bone-like nature, resembling that of a newly formed woven bone tissue.^{30,31} Such increase is in accordance with *in vivo* studies, in which strontium ranelate treatment led to an improvement in volume and microarchitecture of the new bone tissue formed around titanium implants, increasing thus implant osseointegration.²⁵⁻²⁷

Different substrates were used to provide an overall analysis of the influence of strontium ranelate on cell behavior, allowing us to show the effects of treatment in different experimental conditions. When treated with strontium ranelate, the cells cultured on the biomaterials showed an increased proliferation rate, differentiation into mature osteoblasts, and production of mineralized matrix. These changes in the behavior of the osteoblastic cells were seen in all the substrates we used, indicating that strontium ranelate had a similar

effect on all the substrates we used, indicating that strontium ranelate had a similar

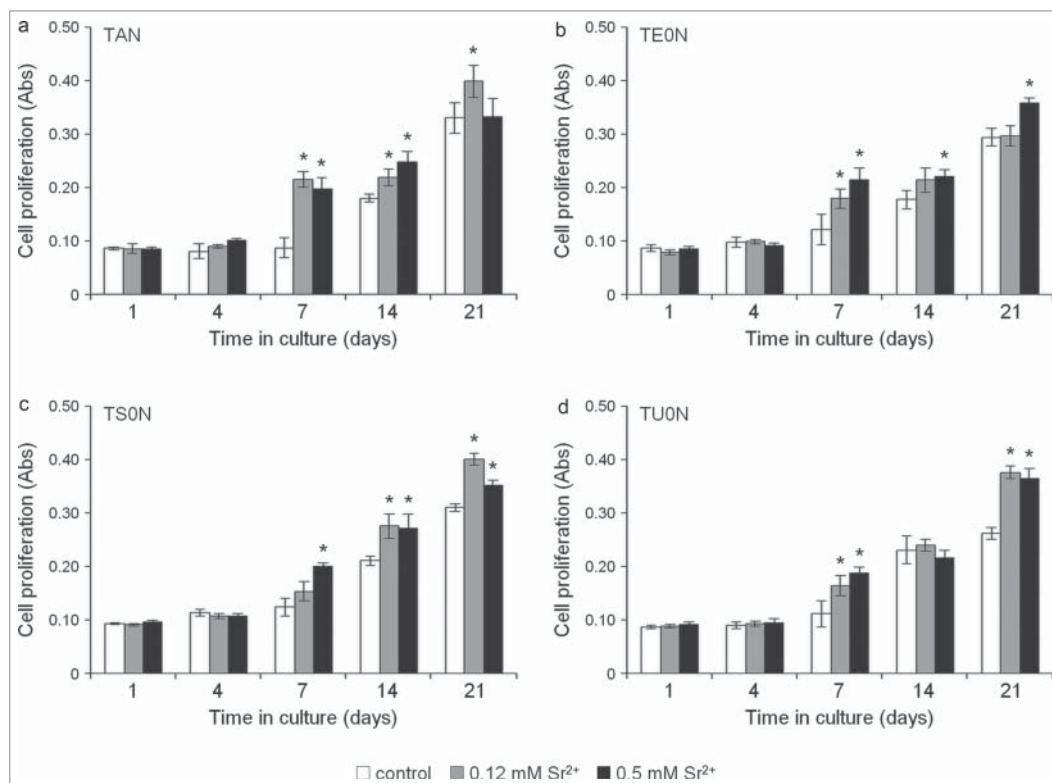


Figure 6. Cell proliferation assay. Live cells were monitored over time with the PrestoBlue Cell Viability Reagent. An increase in cell proliferation was seen in both treated samples in all substrates, particularly from day 7 to 21. After 7 days, this increase was quite consistent for both concentrations of the drug. In some cases, an increase in proliferation was seen only in cells treated with either 0.12 or 0.5 mM Sr²⁺. A large effect size was found for the increase seen on all the substrates ($r > 0.5$). * $P < 0.05$ vs. control.

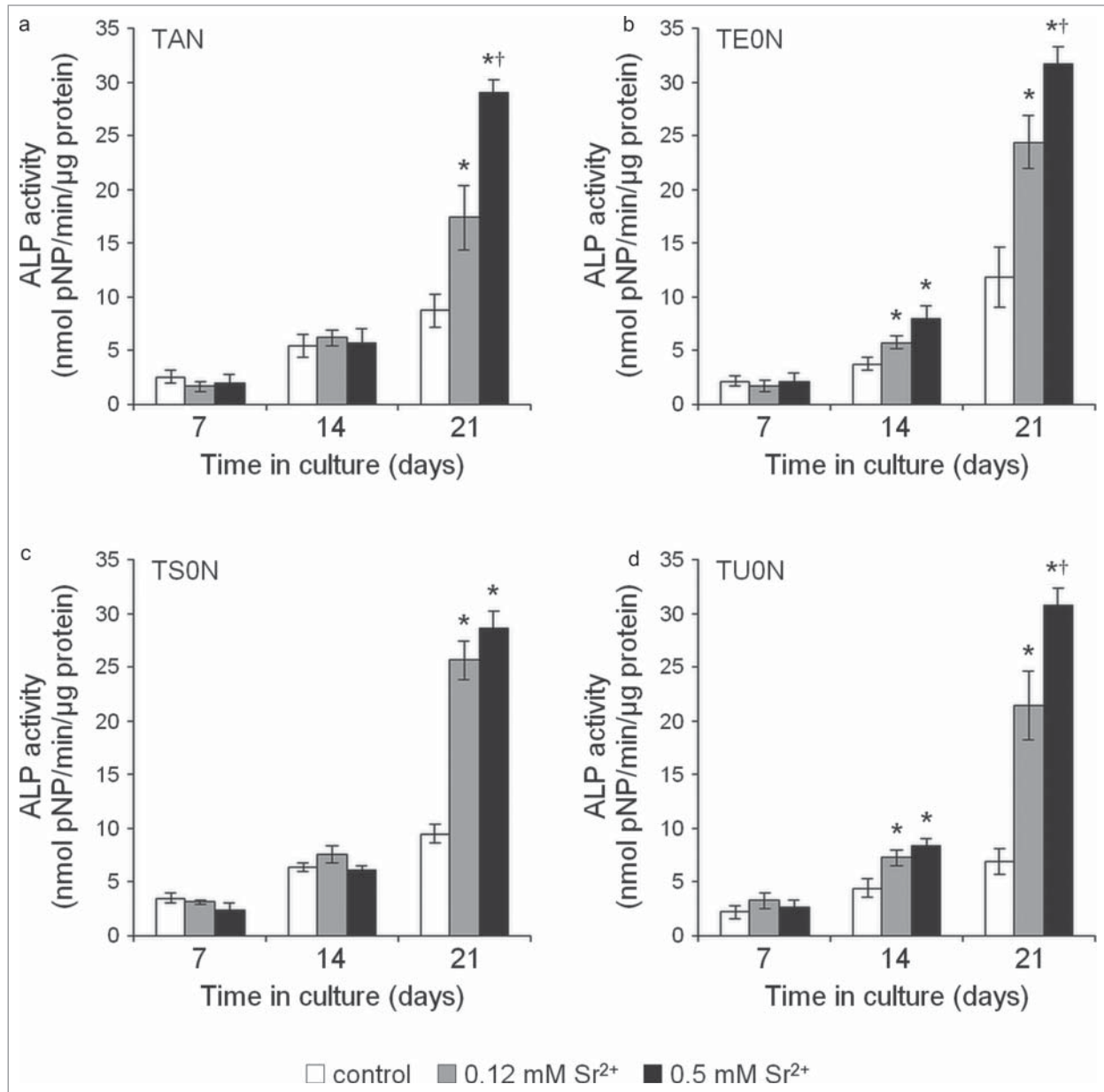


Figure 7. Cell differentiation assay. ALP activity was analyzed in the cell culture medium by quantifying the hydrolysis of pNPP to pNP/min/μg of total protein. A clear increase in ALP activity was seen in treated samples in all substrates, especially after 21 days, indicating an increase in the differentiation of cells into mature osteoblasts. This observed increase showed a large effect size on all the substrates ($r > 0.5$). * $P < 0.05$ vs. control. † $P < 0.05$ vs. 0.12 mM Sr²⁺.

effect in cells cultured on the titanium substrates with 4 different surface topographies. Indeed, the overall magnitude of the observed effects was similar among the substrates, showing that surface topography did not modulate the effects of strontium ranelate on cell behavior.

These results highlight a potential of strontium ranelate for improving the efficacy of orthopedic implants and bone tissue engineering approaches. The direct effects of the drug on enhancing the formation of bone tissue on the surface of biomaterials may play a relevant role on creating a proper cell/matrix/material interface to the integration of the biomaterial

into the regenerated tissue.^{1,2} In this context, we can speculate that this effect of strontium ranelate could be particularly beneficial to patients with osteoporosis, in which the osseointegration of bone implants is quite inadequate.³²⁻³⁴ For instance, in cases in which patients with osteoporosis suffer bone fractures and need bone implants, treatment with strontium ranelate can be useful not only to prevent further fractures, but also to help to overcome some negative effects of osteoporosis on the clinical success of the implants. This reasoning is in agreement with previous findings described in ovariectomized rats.²⁵

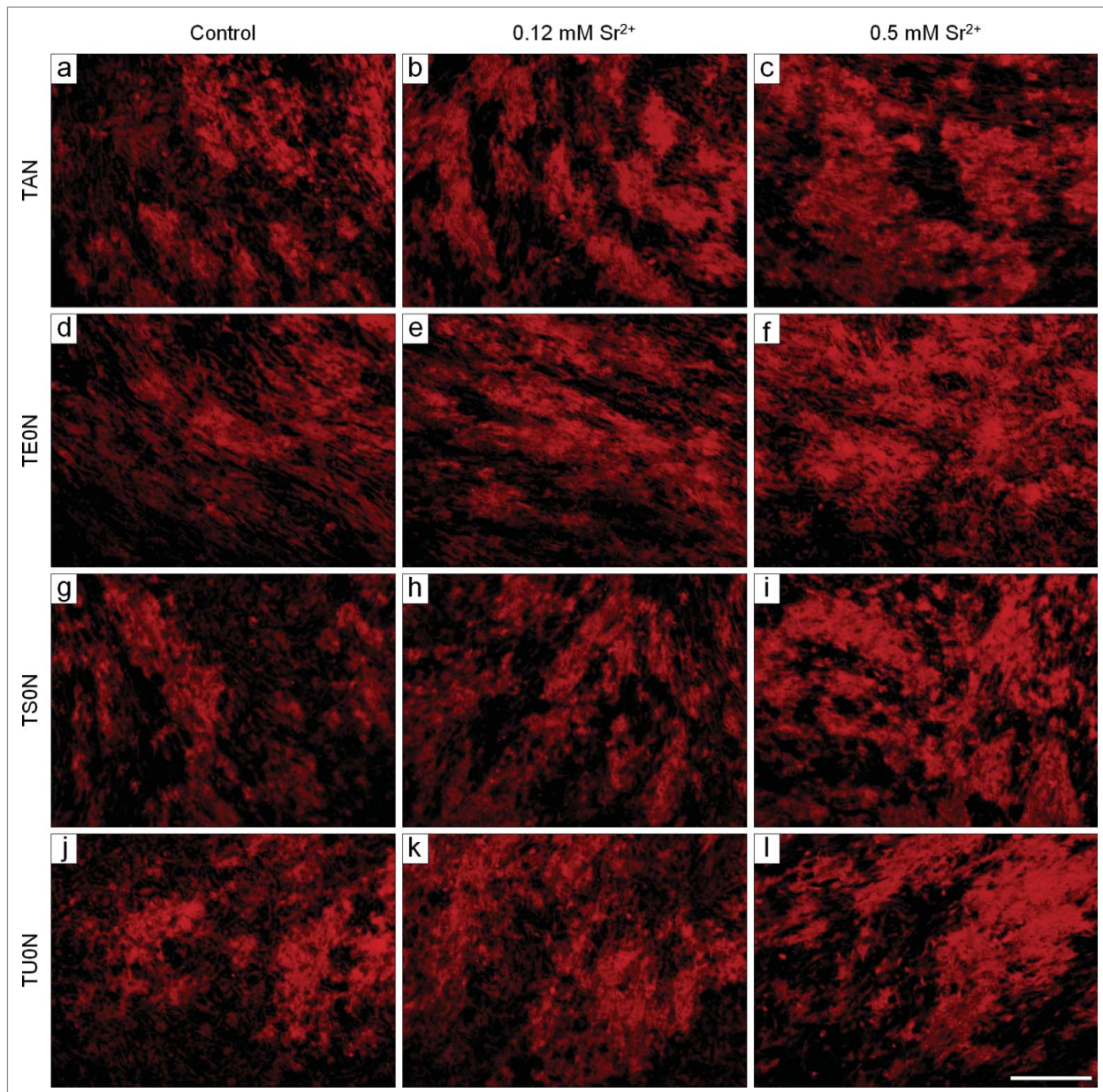


Figure 8. Fluorescence micrographs of the mineralized matrix stained with Alizarin red. Cells were cultured under mineralizing conditions for 28 days. Typical mineralized nodules were observed in all analyzed conditions. They seemed more developed in the treated samples, especially in those treated with 0.5 mM Sr^{2+} . Scale bar: 100 μm .

Finally, it is important to consider the doses of strontium ranelate used in the present study. The dose of 0.12 mM Sr^{2+} was chosen based on the Sr^{2+} levels found in the blood serum of postmenopausal women with osteoporosis treated with 2g of oral strontium ranelate per day for 3 years.³⁵ The dose of 0.5 mM Sr^{2+} was used to access a dose effect of the drug. The dose effect on cell proliferation was quite variable. For instance, for different times in culture or substrates, we could find an increase in proliferation in both treated samples or only in those treated with either 0.12 or 0.5 mM Sr^{2+} . On the other hand, a dose-dependent effect was typically seen in cell differentiation and in the

production of mineralized matrix, with a marked increase often found even after treatment with 0.12 mM Sr^{2+} .

Some limitations of this study should also be considered. For instance, the murine F-OST cells used in this study were chosen because of their typical osteoblastic features, including the ability to produce a bone-like mineralized matrix in culture.^{36,37} Although the use of this cell allowed evaluating different effects of strontium ranelate on the interaction of osteoblastic cells with titanium substrates, these effects should also be analyzed using human osteoblasts. Moreover, it would be interesting to analyze how the drug affects osteoblasts derived from osteoporotic bone

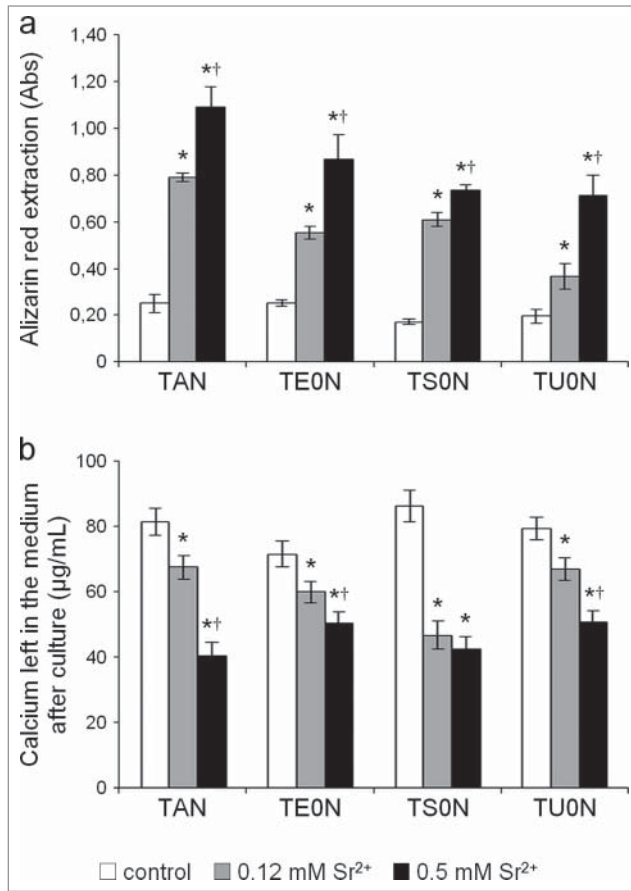


Figure 9. Quantification of the mineralized matrix. (A) The extraction of Alizarin red from the stained samples showed a marked dose-dependent increase in the formation of mineralized matrix in all substrates. (B) The concentration of calcium left in the medium after culture was clearly lower in treated samples in all substrates. This is in accordance with the increase of calcium phosphate minerals deposited on the matrix. This increase in mineralization showed a large effect size on all the substrates ($r > 0.5$). * $P < 0.05$ vs. control. † $P < 0.05$ vs. 0.12 mM Sr²⁺.

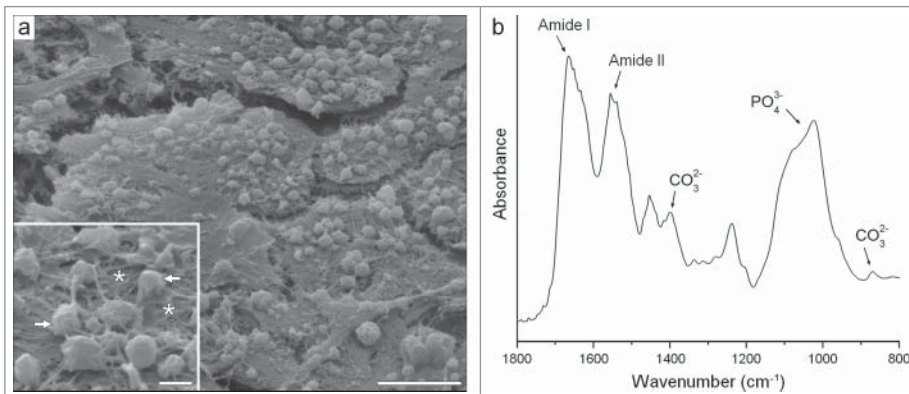


Figure 10. Typical characteristics of the bone-like matrix produced in all analyzed conditions. (A) Scanning electron micrograph. The well-developed cell layers were seen along with numerous globular accretions (see arrows in the inset) associated with an extensive mesh of randomly oriented fibrils (see asterisks in the inset). (B) FTIR spectra. Note bands of PO₄³⁻ and CO₃²⁻ from the carbonated apatite mineral and of Amide I and II from the organic matrix proteins. Scale bar: (a) 10 µm; (inset) 2 µm.

instead of from healthy bone. The presence of osteoclasts in the cell culture systems would also be valuable to analyze a combined effect of the drug on bone formation and resorption on the surface of biomaterials.

A point that should also be considered is that treatment with strontium ranelate is known to lead to the incorporation of Sr²⁺ into the forming bone mineralized matrix.^{38,39} This incorporation occurs with Sr²⁺ partially replacing Ca²⁺ in the apatite crystal lattice, which can cause several changes in the composition and crystal structure of the bone mineral.^{40,41} For this reason, it may be relevant to evaluate in further studies possible changes caused by strontium ranelate in the quality of the interaction between the mineralized matrix and the biomaterial surface at the bone apatite crystal level (i.e., at the nanoscale).

Conclusions

Strontium ranelate improved the interaction of osteoblastic cells with different titanium substrates. We show that treatment preserved cell shape and the orientation of cells on grooved surfaces, with no changes found also in the initial cell adhesion to the substrates. We found, however, that treatment increased cell proliferation and differentiation into mature osteoblasts and the production of bone-like mineralized matrix in all substrates. The overall magnitude of these effects was similar among the different substrates. Finally, our results indicate that strontium ranelate may improve implant osseointegration by acting directly on osteoblastic cells, playing a promising role on enhancing the clinical success of bone implants, particularly in patients with osteoporosis.

Materials and methods

Titanium substrates

The substrates were made of pure titanium and had 4 different surface topographies, obtained using acid etching (TAN), electro-erosion processing (TEON), sand-blasting (TSON), and machine-tooling (TUON). All substrates had similar roughness amplitudes ($S_a = 0.7 \mu\text{m}$). In particular, the TUON substrates presented parallel grooves for analyzing contact guidance of the cells. Scanning electron micrographs of each of the surfaces were taken with a FEI Quanta 400 microscope (Figs. 1A-D). A detailed characterization can be found elsewhere.^{42,43}

Cell culture

The cells used in this study were F-OST osteoblasts, previously isolated from the femoral endosteal region of

8–12 weeks old male BALB/c mice³⁸ and cryopreserved in liquid nitrogen to be used in future studies. They present high alkaline phosphatase (ALP) activity, produce typical bone matrix proteins (e.g., type I collagen, bone sialoprotein, and osteopontin), and spontaneously form mineralized nodules under basal culture conditions.³⁶ The matrix produced by these cells in culture show many typical bone-like characteristics.³⁷ The cells were seeded onto the titanium substrates at a density of 2.0×10^4 cells/sample in 24-well plates. Before placing the substrates in the plates, the wells were coated with a 2% agar gel to avoid cell adhesion on their bottom. Cells were cultured in Dulbecco's Modified Eagle Medium containing 10% fetal bovine serum and antibiotics (100 U/mL of penicillin and 100 µg/mL of streptomycin). For the mineralization assay, cells were cultured in medium with 50 µg/mL of ascorbic acid and 2 mM of β-glycerophosphate. The medium was changed twice a week. Cells were treated during the whole culture time with strontium ranelate (PROTOS[®] 2g, Servier) added to the medium at 0.12 and 0.5 mM Sr²⁺. The control used for each of the titanium substrates were cell cultures that were not treated with strontium ranelate.

Fluorescent labeling of the cells

After culture, samples were fixed with 2% paraformaldehyde for 30 min, permeabilized with 0.2% Triton X-100 for 15 min, and incubated with 1% albumin solution for 20 min to block nonspecific protein binding sites. The samples were then incubated with 0.4 µg/mL of FITC-phalloidin for 60 min to label the actin cytoskeleton of the cells and with 100 ng/mL of DAPI for 20 min to label the cell nuclei. After each of the described steps, samples were washed 3 times with phosphate buffered saline (PBS). The labeled cells were observed with an Olympus BX51 epifluorescence microscope.

Image analysis

Fluorescence images were analyzed with the ImageJ software (version 1.47v).⁴⁴ In order to evaluate the shape of cells, we carefully traced the outlines of individual cells labeled with FITC-phalloidin after 24 hours in culture and measured their area and shape descriptors – aspect ratio, circularity, and solidity. Briefly, the aspect ratio is calculated as the major/minor axes of the best fitting ellipse, with values increasing from 1.0 indicating an elongation of the cells. Circularity is obtained by calculating $4\pi \times \text{area}/\text{perimeter}^2$, with a value of 1.0 indicating a perfect circle. Solidity is the area/(convex area), showing values decreasing from 1.0 in cells with irregular shapes and distinct prolongations.

To analyze the orientation of the cells, we measured the smallest angle between the major axis of their best fitting ellipse and the direction of the grooves in TU0N substrates, obtaining values ranging from 0° (perfectly aligned) to 90° (exactly perpendicular). At least 60 individual cells were examined for each analyzed condition. The number of cells on the substrates after 4 and 24 hours in culture was determined by counting the nuclei labeled with DAPI per field using a 10× objective lens. At least 30 fields were examined for each analyzed condition.

Cell proliferation

Cells were analyzed after 1, 4, 7, 14, and 21 days with the PrestoBlue[®] Cell Viability Reagent (Life Technologies). This reagent is a resazurin-based solution that allows monitoring living cells over time and quantitatively measure their proliferation. Briefly, cells were incubated with the PrestoBlue solution for 60 min at 37°C in the dark. The solutions were then collected and the absorbance was measured at 570 nm with 595 nm as a reference wavelength using a microplate reader. Each sample was analyzed in triplicate.

Cell differentiation

Osteoblastic cell differentiation was investigated after 7, 14, and 21 days by measuring the ALP activity in the cell culture medium. Samples were analyzed using p-nitrophenyl phosphate (pNPP) as a colorimetric substrate for ALP. Briefly, samples were incubated with 1 mg/mL of p-NPP in 1 M diethanolamine buffer for 10 min and absorbance was measured at 405 nm using a microplate reader. Each sample was analyzed in triplicate. Standards were used to determine the concentration of p-nitrophenol (pNP, product of pNPP hydrolysis) and Coomassie Plus[™] (Bradford) Assay Kit (Thermo Scientific Pierce) was used for total protein quantitation. Results were expressed as nmol of pPN produced per min per µg of protein.

Alizarin red staining and quantification

Cells were cultured with mineralizing medium for 28 days, fixed with 2% paraformaldehyde for 30 min, and washed with PBS. They were then stained with a 2% Alizarin red solution for 10 min and washed extensively with distilled water. Images of the mineralized matrix were taken with an Olympus BX51 epifluorescence microscope. The mineralized matrix was quantified by extracting the Alizarin red from the samples using cetylpyridinium chloride (CPC). Briefly, the stained samples were incubated with 10% w/v CPC in 10 mM sodium phosphate buffer under sonication for 3 hours. The solutions were then collected and the solubilized Alizarin red was quantified by measuring the absorbance at 550 nm using a microplate reader. Each sample was analyzed in triplicate.

Quantification of calcium in the medium

At the end of the 28 days of the mineralization assays, the cell culture medium was collected and analyzed using an arsenazo III method with the Calcium AS FS kit (DiaSys Diagnostic Systems) to quantify the concentration of calcium left in the medium after culture. This was done to indirectly assess the amount of calcium deposited in the mineralized matrix. Briefly, samples were incubated with the reagent for 5 min and absorbance was measured at 650 nm using a microplate reader. The absorbance values were adjusted to µg/mL of calcium using a standard solution curve. Each sample was analyzed in triplicate.

Scanning electron microscopy

After 28 days in culture, the mineralized samples were fixed with 4% glutaraldehyde and 2% paraformaldehyde in 0.1 M phosphate buffer for 30 min and washed 3 times with PBS.

They were then dehydrated in increasing ethanol solutions (50, 70, 80, 95, and 100%), with 3 5-min baths per solution. Hexamethyldisilazane (HMDS) was used for drying the samples. Finally, the samples were sputter coated with gold and observed by scanning electron microscopy (SEM) with a FEI Quanta 400 microscope.

Fourier transform infrared spectroscopy

Before the gold coating, the samples described above for SEM were analyzed by Fourier transform infrared spectroscopy (FTIR) with a Bruker IFS 66/S spectrometer combined to a Bruker IRScope-1 microscope. Absorption spectra were acquired by averaging 128 scans at a resolution of 4 cm^{-1} using the attenuated total reflection (ATR) mode, which allows analyzing samples directly without damaging them.

Statistical analyses

Statistical analyses were carried out using the SPSS® Statistics software (version 20; IBM). Data are presented as mean \pm 95% confidence interval. Kruskal-Wallis test (nonparametric ANOVA) was used for the overall comparison among the control and treatment groups. In cases in which we found a significant

difference, we further compared each treatment group with the control using the Mann-Whitney test. Differences were considered significant when $P < 0.05$. In order to compare the magnitude of the effects of strontium ranelate seen on the different substrates, we measured the effect size r , considering the standardized estimates of $r > 0.5$ for a large effect, $r \approx 0.3\text{--}0.5$ for a medium effect, and $r < 0.3$ for a small effect.^{45,46}

Disclosure of Potential Conflicts of Interest

No potential conflicts of interest were disclosed.

Acknowledgments

We thank Stephan Knopf and Simon Gree for their technical assistance in SEM and FTIR analysis, respectively.

Funding

This study was supported by FAPERJ, CNPq, and Inmetro (Brazil) and by the CAPES/COFECUB program no. 628/09 (Brazil/France cooperation).

References

1. Anselme K. Osteoblast adhesion on biomaterials. *Biomaterials*. 2000; 21(7):667-81; PMID:10711964; [http://dx.doi.org/10.1016/S0142-9612\(99\)00242-2](http://dx.doi.org/10.1016/S0142-9612(99)00242-2)
2. Anselme K. Biomaterials and interface with bone. *Osteoporos Int*. 2011; 22(6):2037-42; PMID:21523393; <http://dx.doi.org/10.1007/s00198-011-1618-x>
3. Davies JE. Mechanisms of endosseous integration. *Int J Prosthodont*. 1998; 11(5):391-401; PMID:9922731
4. Davies JE. Understanding peri-implant endosseous healing. *J Dent Educ*. 2003; 67(8):932-49; PMID:12959168
5. Anselme K, Ponche A, Bigerelle M. Relative influence of surface topography and surface chemistry on cell response to bone implant materials. Part 2: biological aspects. *Proc Inst Mech Eng H*. 2010; 224(12):1487-507; PMID:21287833; <http://dx.doi.org/10.1243/09544119JEM901>
6. Ponche A, Bigerelle M, Anselme K. Relative influence of surface topography and surface chemistry on cell response to bone implant materials. Part 1: physico-chemical effects. *Proc Inst Mech Eng H*. 2010; 224(12):1471-86; PMID:21287832; <http://dx.doi.org/10.1243/09544119JEM900>
7. Frenkel SR, Simon J, Alexander H, Dennis M, Ricci JL. Osseointegration on metallic implant surfaces: effects of microgeometry and growth factor treatment. *J Biomed Mater Res*. 2002; 63(6):706-13; PMID:12418014; <http://dx.doi.org/10.1002/jbm.10408>
8. Zhou F, Yuan L, Huang H, Chen H. Phenomenon of "contact guidance" on the surface with nano-micro-groove-like pattern and cell physiological effects. *Chinese Sci Bull*. 2009; 54(18):3200-5; <http://dx.doi.org/10.1007/s11434-009-0366-1>
9. Hing KA. Bone repair in the twenty-first century: biology, chemistry or engineering? *Philos Trans A Math Phys Eng Sci*. 2004; 362(1825):2821-50; PMID:15539372; <http://dx.doi.org/10.1098/rsta.2004.1466>
10. Ikada Y. Challenges in tissue engineering. *J R Soc Interface*. 2006; 3(10):589-601; PMID:16971328; <http://dx.doi.org/10.1098/rsif.2006.0124>
11. Navarro M, Michiardi A, Castano O, Planell JA. Biomaterials in orthopaedics. *J R Soc Interface*. 2008; 5(27):1137-58; PMID:18667387; <http://dx.doi.org/10.1098/rsif.2008.0151>
12. Wozney JM, Rosen V. Bone morphogenetic protein and bone morphogenetic protein gene family in bone formation and repair. *Clin Orthop Relat Res*. 1998; 346:26-37; PMID:9577407
13. Sumner DR, Turner TM, Urban RM, Turek T, Seeherman H, Wozney JM. Locally delivered rhBMP-2 enhances bone ingrowth and gap healing in a canine model. *J Orthop Res*. 2004; 22(1):58-65; PMID:14656660; [http://dx.doi.org/10.1016/S0736-0266\(03\)00127-X](http://dx.doi.org/10.1016/S0736-0266(03)00127-X)
14. Hunziker EB, Enggist L, Küffer A, Buser D, Liu Y. Osseointegration: the slow delivery of BMP-2 enhances osteoinductivity. *Bone*. 2012; 51(1):98-106; PMID:22534475; <http://dx.doi.org/10.1016/j.bone.2012.04.004>
15. Ammann P. Strontium ranelate: a novel mode of action leading to renewed bone quality. *Osteoporos Int*. 2005 Jan; Suppl 1:S11-5; PMID:15578157
16. Bonnelye E, Chabadel A, Saltel F, Jurdic P. Dual effect of strontium ranelate: stimulation of osteoblast differentiation and inhibition of osteoclast formation and resorption in vitro. *Bone*. 2008; 42(1):129-38; PMID:17945546; <http://dx.doi.org/10.1016/j.bone.2007.08.043>
17. Marie PJ, Felsenberg D, Brandi ML. How strontium ranelate, via opposite effects on bone resorption and formation, prevents osteoporosis. *Osteoporos Int*. 2011; 22(6):1659-67; PMID:20812008; <http://dx.doi.org/10.1007/s00198-010-1369-0>
18. Canalis E, Hott M, Deloffre P, Tsouderos Y, Marie PJ. The divalent strontium salt S12911 enhances bone cell replication and bone formation in vitro. *Bone*. 1996; 18(6):517-23; PMID:8805991; [http://dx.doi.org/10.1016/8756-3282\(96\)00080-4](http://dx.doi.org/10.1016/8756-3282(96)00080-4)
19. Caverzasio J. Strontium ranelate promotes osteoblastic cell replication through at least two different mechanisms. *Bone*. 2008; 42(6):1131-6; PMID:18378206; <http://dx.doi.org/10.1016/j.bone.2008.02.010>
20. Barbara A, Delannoy P, Denis BG, Marie PJ. Normal matrix mineralization induced by strontium ranelate in MC3T3-E1 osteogenic cells. *Metabolism*. 2004; 53(4):532-7; PMID:15045704; <http://dx.doi.org/10.1016/j.metabol.2003.10.022>
21. Choudhary S, Halbout P, Alander C, Raisz L, Pilbeam C. Strontium ranelate promotes osteoblastic differentiation and mineralization of murine bone marrow stromal cells: involvement of prostaglandins. *J Bone Miner Res*. 2007; 22(7):1002-10; PMID:17371157; <http://dx.doi.org/10.1359/jbmr.070321>
22. Querido W, Farina M. Strontium ranelate increases the formation of bone-like mineralized nodules in osteoblast cell cultures and leads to Sr incorporation into the intact nodules. *Cell Tissue Res*. 2013; 354(2):573-80; PMID:23774883; <http://dx.doi.org/10.1007/s00441-013-1669-8>
23. Reginster JY, Felsenberg D, Boonen S, Diez-Perez A, Rizzoli R, Brandi ML, Spector TD, Brixen K, Goemaere S, Cormier C, et al. Effects of long-term strontium ranelate treatment on the risk of nonvertebral and vertebral fractures in postmenopausal osteoporosis: Results of a five-year, randomized, placebo-controlled trial. *Arthritis Rheum*. 2008; 58(6):1687-95; PMID:18512789; <http://dx.doi.org/10.1002/art.23461>
24. Meunier PJ, Roux C, Ortolani S, Diaz-Curiel M, Compston J, Marquis P, Cormier C, Isaia G, Badurski J, Wark JD, et al. Effects of long-term strontium ranelate treatment on vertebral fracture risk in postmenopausal women with osteoporosis. *Osteoporos Int*. 2009; 20(10):1663-73; PMID:19153678; <http://dx.doi.org/10.1007/s00198-008-0825-6>
25. Li Y, Feng G, Gao Y, Luo E, Liu X, Hu J. Strontium ranelate treatment enhances hydroxyapatite-coated titanium screws fixation in osteoporotic rats. *J Orthop Res*. 2010; 28(5):578-82; PMID:20014319
26. Maïmoun L, Brennan TC, Badoud I, Dubois-Ferriere V, Rizzoli R, Ammann P. Strontium ranelate improves implant osseointegration. *Bone*. 2010; 46(5):1436-41; <http://dx.doi.org/10.1016/j.bone.2010.01.379>
27. Li Y, Li X, Song G, Chen K, Yin G, Hu J. Effects of strontium ranelate on osseointegration of titanium implant in osteoporotic rats. *Clin Oral Implants Res*. 2012; 23(9):1038-44; PMID:22117625; <http://dx.doi.org/10.1111/j.1600-0501.2011.02252.x>
28. Aubin JE. Advances in the osteoblast lineage. *Biochem Cell Biol*. 1998; 76(6):899-910; PMID:10392704; <http://dx.doi.org/10.1139/o99-005>
29. Golub EE, Boesze-Battaglia K. The role of alkaline phosphatase in mineralization. *Curr Opin Orthop*.

- 2007; 18:444-8; <http://dx.doi.org/10.1097/BCO.0b013e3282630851>
30. Weiner S, Wagner HD. The material bone: structure-mechanical function relations. *Ann Rev Mat Sci.* 1998; 28:271-98; <http://dx.doi.org/10.1146/annurev.matsci.28.1.271>
 31. Dorozhkin SV. Calcium orthophosphates in nature, biology and medicine. *Materials.* 2009; 2:399-498; <http://dx.doi.org/10.3390/ma2020399>
 32. Marco F, Milena F, Gianluca G, Vittoria O. Peri-implant osteogenesis in health and osteoporosis. *Micron.* 2005; 36(7-8):630-44; PMID:16182543; <http://dx.doi.org/10.1016/j.micron.2005.07.008>
 33. Pesce V, Speciale D, Sammarco G, Patella S, Spinarelli A, Patella V. Surgical approach to bone healing in osteoporosis. *Clin Cases Miner Bone Metab.* 2009; 6(2):131-5; PMID:22461162
 34. Piarulli G, Rossi A, Zatti G. Osseointegration in the elderly. *Aging Clin Exp Res.* 2013; 25 Suppl 1:S59-60; <http://dx.doi.org/10.1007/s40520-013-0103-0>
 35. Meunier PJ, Roux C, Seeman E, Ortolani S, Badurski JE, Spector TD, Cannata J, Balogh A, Lemmel EM, Pors-Nielsen S, et al. The effects of strontium ranelate on the risk of vertebral fracture in women with postmenopausal osteoporosis. *N Engl J Med.* 2004; 350(5):459-68; PMID:14749454; <http://dx.doi.org/10.1056/NEJMoa022436>
 36. Balduino A, Hurtado SP, Frazão P, Takiya CM, Alves LM, Nasciutti LE, El-Cheikh MC, Borojevic R. Bone marrow subendosteal microenvironment harbours functionally distinct haemosupportive stromal cell populations. *Cell Tissue Res.* 2005; 319(2):255-66; PMID:15578225; <http://dx.doi.org/10.1007/s00441-004-1006-3>
 37. Querido W, Abraçado LG, Rossi AL, Campos APC, Rossi AM, San Gil RAS, Borojevic R, Balduino A, Farina M. Ultrastructural and mineral phase characterization of the bone-like matrix assembled in F-OST osteoblast cultures. *Calcif Tissue Int.* 2011; 89(5):358-71; PMID:21901516; <http://dx.doi.org/10.1007/s00223-011-9526-9>
 38. Oliveira JP, Querido W, Caldas RJ, Campos AP, Abraçado LG, Farina M. Strontium is incorporated in different levels into bones and teeth of rats treated with strontium ranelate. *Calcif Tissue Int.* 2012; 91(3):186-95; PMID:22806682; <http://dx.doi.org/10.1007/s00223-012-9625-2>
 39. Li C, Paris O, Siegel S, Roschger P, Paschalis EP, Klaushofer K, Fratzl P. Strontium is incorporated into mineral crystals only in newly formed bone during strontium ranelate treatment. *J Bone Miner Res.* 2010; 25(5):968-75; PMID:19874195
 40. Querido W, Campos AP, Martins Ferreira EH, San Gil RA, Rossi AM, Farina M. Strontium ranelate changes the composition and crystal structure of the biological bone-like apatite produced in osteoblast cell cultures. *Cell Tissue Res.* 2014; 357(3):793-801; PMID:24859219; <http://dx.doi.org/10.1007/s00441-014-1901-1>
 41. Rossi AL, Moldovan S, Querido W, Rossi A, Werckmann J, Ersen O, Farina M. Effect of strontium ranelate on bone mineral: Analysis of nanoscale compositional changes. *Micron.* 2014; 56:29-36; PMID:24207060; <http://dx.doi.org/10.1016/j.micron.2013.09.008>
 42. Bigerelle M, Anselme K. Statistical correlation between cell adhesion and proliferation on biocompatible metallic materials. *J Biomed Mater Res A.* 2005; 72(1):36-46; PMID:15558592; <http://dx.doi.org/10.1002/jbm.a.30212>
 43. Anselme K, Bigerelle M. Topography effects of pure titanium substrates on human osteoblast long-term adhesion. *Acta Biomater.* 2005; 1(2):211-22; PMID:16701798; <http://dx.doi.org/10.1016/j.actbio.2004.11.009>
 44. Schneider CA, Rasband WS, Eliceiri KW. NIH Image to ImageJ: 25 years of image analysis. *Nat Methods.* 2012; 9(7):671-5; PMID:22930834; <http://dx.doi.org/10.1038/nmeth.2089>
 45. Field A. *Discovering statistics using SPSS.* 3rd ed. London: SAGE Publications; 2009
 46. Maher JM, Markey JC, Ebert-May D. The other half of the story: effect size analysis in quantitative research. *CBE Life Sci Educ.* 2013; 12(3):345-51; PMID:24006382